九州大学学術情報リポジトリ
Kyushu University Institutional Repository

Development of Models to Predict Flexural Strength of 3D Printed Specimens in Terms of Input Parameters

Singh, Manohar
U.S.I.C.T., Guru Gobind Singh Indraprastha University

Pushpendra S. Bharti
U.S.I.C.T., Guru Gobind Singh Indraprastha University

https://doi.org/10.5109/7183438

出版情報：Evergreen. 11 (2), pp.1292-1298, 2024-06. 九州大学グリーンテクノロジー研究教育センター
バージョン：
権利関係：Creative Commons Attribution 4.0 International

KYUSHU UNIVERSITY

Development of Models to Predict Flexural Strength of 3D Printed Specimens in Terms of Input Parameters

Manohar Singh[1,2*], Pushpendra S. Bharti[1]

[1]U.S.I.C.T., Guru Gobind Singh Indraprastha University, Delhi-110078, India

[2]Galgotias College of Enggineering and Technology, Greater Noida, U.P.-201310,India

*Author to whom correspondence should be addressed:

E-mail: manoharmnr@gmail.com

(Received September 14, 2022: Revised April 8, 2024: Accepted June 14, 2024).

Abstract: In the present work, models have been generated for prediction of flexural strength, in terms of four input parameters i.e. temperature of the extruder, density of the infill, printing speed, and layer height, for 3D printed samples prepared using the Fused Deposition Modelling (FDM) technique. The filament used for printing the specimen is that of Poly Lactic Acid (PLA). Regression and Artificial Neural Networks (ANN) have been used to build mathematical models by utilizing the experimental data obtained for Taguchi L16 Orthogonal array. Value of R-square for regression is 86.92. Additionally, the percentage deviation between experimental values and model predicted values have been calculated as per ANN model and the variation is 4.06 percent. Hence ANN model can be used for determination of flexural strength for any combination of four input parameters under study.

Keywords: Fused deposition modeling (FDM); Poly Lactic Acid (PLA); Artificial Neural Network (ANN)

1. Introduction

There has been a gradual increase in the use of Rapid prototyping technology in industry in recent past. Rapid prototyping procedures, such as three-dimensional (3D) printing, is a type of technique that creates 3D objects directly by adding material layers rather than removing it. As opposed to traditional machining methods, which necessitate special tools, additive manufacturing uses a layering of materials to create parts[1)] from 3D CAD model data. At the same time, additive manufacturing has grown in popularity as a means of producing goods faster while also saving money. Fused deposition modelling (FDM), commonly referred to as fused filament fabrication, is the most prevalent additive manufacturing (AM) technology (FFF). This is owing to the wide range of commercially accessible materials, inexpensive accessibility, and ease of usage. Due to decreased material waste and ability to fabricate complex geometries, these kinds of technologies have the ability to save considerable amounts of money. As a result, they've attracted a lot of attention in the last few decades. Creation of 3D object is accomplished due to adhesion of layers of hot semi-melted thermoplastic material extruded from nozzle of an FFF printer. A heated print head emits a steady stream of the semi-molten plastic during this operation. The deposited material hardens practically immediately after it leaves the heated print head, resulting in the desired product appearing in a short span of time. As FFF machines have become more widely available, researchers have been motivated to work on understanding the structural performance of parts made using this technology.

Numerous researches have been conducted in the last several years to ascertain the influence of input variables on various mechanical properties. Input factors investigated include infill density, nozzle diameter, annealing temperature, feed rate, layer height, printing speed, raster angle, raster width, contour number, air gap, contour width, and build orientation. Dhinesh et. al.[2)] found that when it comes to tensile strength, PLA outperforms ABS which further improves for 80% PLA and 20% ABS mixture. As far as flexural strength is considered 50% each of PLA and ABS shows better result. This opens the door for further study that can be carried out for various % combination of PLA and ABS. Singh et. al.[3)] studied the PLA reinforced with chitosan and found Tensile and flexural strengths decrease as the chitosan weight percentage increases. while compressive strength increased. Zandi et. al.[4)] evaluated layer thickness as most significant variable influencing the flexural strength for wood PLA composite. Gunaya et. al.[5)] found infilled density to be most vital parameter impacting the mechanical characteristics of PLA+ samples. Both flexural and tensile strength were higher for 0 or 90 degree orientation and decreased with increase in print speed. For PLA-graphene samples, Camargo et. al.[6)] reported

improvement in mechanical properties with increase in layer height. Rajpurohit et. al.[7] ascertained layer thickness as main variable to affect the flexural strength most and inversely. Raster width and angles were the factors which have influence on flexural strength of specimen printed of ULTEM9085 using FDM which was revealed by Gebisa et. al.[8] Chacon et. al.[9] suggested on edge orientation for optimal mechanical properties like flexural and tensile strength. Samples prepared from ABS P430 were examined by Hernandez[10] and samples printed in 0 degrees depicted better tensile strength while 0-degree print resulted in samples with higher flexural strength. Response surface analysis for optimal parameter combination for tensile and flexural strength has been performed by Sood et. al.[11]

2. Proposed Methodology

The proposed methodology comprises of selection of 3D printer, filament, process parameters, levels of parameters and design of the experiment. Then the flexural strength of printed specimen is measured. Finally obtained data is analyzed by obtaining mathematical model using regression and ANN. Percentage deviation of ANN predicted values as compared to experimental value has been calculated. ANOVA has been used for distinguishing significant and non-significant process parameters while Taguchi has been used for optimization of flexural strength and identification of corresponding parameters. Obtained result has been validated experimentally. The proposed methodology is shown in Fig. 1.

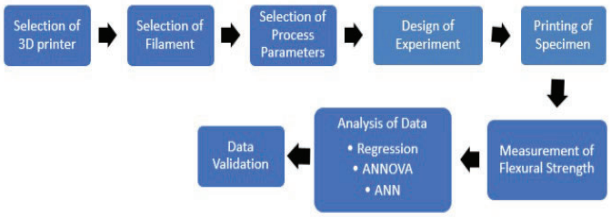

Fig. 1: Proposed Methodology

3. Material & Methods

The flexural specimens have been produced in accordance with ASTM D790 specifications. Autodesk Inventor is used to create the 3D model and convert it to.STL (Stereolithography) file type. Using Flash Print software, the Flash forge Dreamer NX printer's machine parameters have been regulated and slicing has been carried out. Extruder temperature, print speed, infill density and layer thickness are all input parameters that have been adjusted at four different levels. Figure 2 depicts a printed specimen set.

4. Fabrication and Testing

In accordance with the design of experiment, three specimens have been produced for each variation of the L16 orthogonal array. NTF Tensile, Compression, and Flexural Strength Tester was used to test the specimens (Fig. 3). In order to conduct a flexural test, the specimen was placed on two rollers at the bottom and a constant load was delivered, from the top roller at mid-point till failure, at an ever-increasing rate. For each test, the maximum force, maximum flexural strength and maximum elongation have been recorded. The flexural strength of various parameter combinations[12] can be seen in Table 1 where A represents the layer thickness in millimetres, B is the print speed in millimetres per second, C represents percentage of infill density, and D being the temperature of extruder in degrees Celsius.

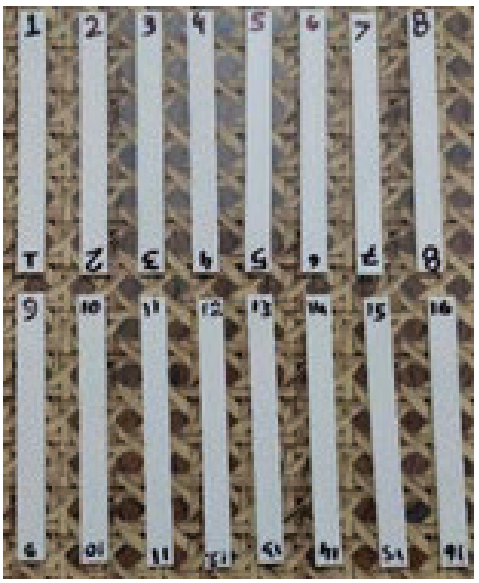

Fig. 2: Printed Samples

Fig. 3: NTF Testing Machine

Table 1. Test results of all samples

Specimen No.	A	B	C	D	Flexural Strength (Kg/mm^2)
1	0.2	50	70	190	14.632
2	0.2	100	80	200	11.836
3	0.2	150	90	210	15.146
4	0.2	200	100	220	16.113
5	0.25	50	80	210	15.962
6	0.25	100	70	220	14.978
7	0.25	150	100	190	3.193
8	0.25	200	90	200	1.729
9	0.3	50	90	220	17.051
10	0.3	100	100	210	12.187
11	0.3	150	70	200	6.006
12	0.3	200	80	190	2.988
13	0.35	50	100	200	14.039
14	0.35	100	90	190	2.754
15	0.35	150	80	220	9.906
16	0.35	200	70	210	4.629

5. Mathematical modelling

Regression analysis and an artificial neural network have been used to generate the mathematical models to monitor and predict the response to changes in input parameters. Once the two methods have developed models, they are compared to see which model is the most accurate. Models have been compared based on how well they predict the results, as detailed in the following sections.

5.1 Regression Modelling

The MINITAB17 software's regression modelling[13] has been utilized to construct a relation between input and output, with 95 as the correction factor. exhibit The derived model and the accompanying ANOVA[14], with an R-sq value at 86.92 percent, is exhibited in equation 1 and table 2 . The P value for the regression model is less than 0.05, which is evident from the ANOVA table. P values less than 0.05 indicate[15] that the input parameters under study i.e. layer thickness, extruder temperature and print speed are important variables and influence the output. Figure 4 illustrates the normal probability plot of the regression analysis. The figure depicts a normal distribution of data over the range indicating that the relation is very much linear as the residuals are distributed normally.

$$Flexural\ Strength = -34.8 - 38.4 \times A - 0.0581 \times B + 0.0296 \times C + 0.2944 \times D \quad (1)$$

Table 2. Analysis of Variance

Source	DF	Adj SS	Adj MS	F-Value	P-Value
Regression	4	417.588	104.397	18.28	0.000
Layer Thickness (A)	1	73.78	73.78	12.92	0.004
Print Speed (B)	1	168.72	168.72	29.54	0.000
Infill Density (C)	1	1.755	1.755	0.31	0.590
Extruder Temperature (D)	1	173.334	173.334	30.34	0.000
Error	11	62.833	5.712		
Total	15	480.422			

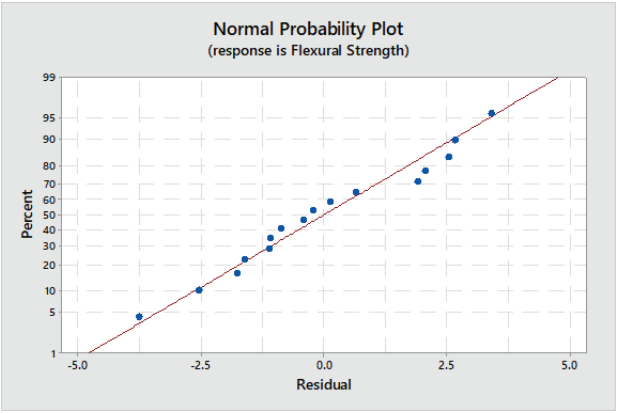

Fig. 4: Normal Probability Plot

5.2 Taguchi Analysis

For the L16 orthogonal array, Taguchi analysis[16] has been performed[17]. Table 3 displays the response for the signal-to-noise ratio for larger the better condition[18]. With regard to flexural strength, it is clear from the table that print speed has the greatest impact on the end result. Figure 5 depicts the main effect curve for signal-to-noise ratio. The greatest flexural strength can be achieved when the at print speed of 50 mm/sec, extruder temperature of 220^{0}C, infill density of 100 % and layer thickness of 0.2 mm.

Table 3. Response table for SN Ratio

Level	(A)	(B)	(C)	(D)
1	23.13	23.74	18.92	12.92
2	15.6	18.87	18.74	16.18
3	17.86	17.29	15.45	20.67
4	16.24	12.93	19.72	23.05
Delta	7.53	10.81	4.27	10.13
Rank	3	1	4	2

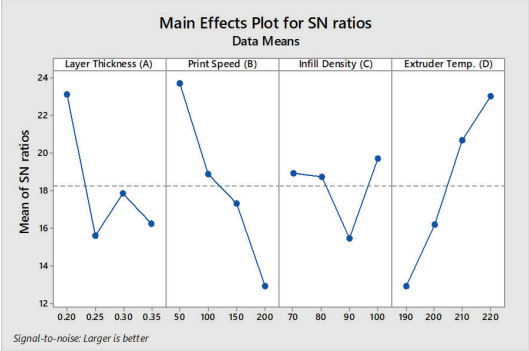

Fig. 5: Main Effect plot for SN ratios

5.3 Artificial Neural Network (ANN) modelling

ANN is based on the way the human brain works, with its many interconnected layers of neurons mapping input to output. An increasing number of scientists are relying on ANN to generate relationships between input and output data points[19]. To begin, a neural network made up of layers of linked neurons, has been created[20]. Neurons and connections are given weights and biases to process the input. Figure 6 depicts the ANN's architecture. A, B, C, and D are all of the input neurons in the Input layer. X, Y, and Z are represented by three neurons in a hidden layer. One neuron in output layer, i.e. layer F. Training and testing were carried out using data generated by the feed-forward back proportion approach, which was used to define the architecture. TANSIG has been selected as the activation function. Data has been trained and tested in an 80:20 ratio, with training taking precedence over testing.

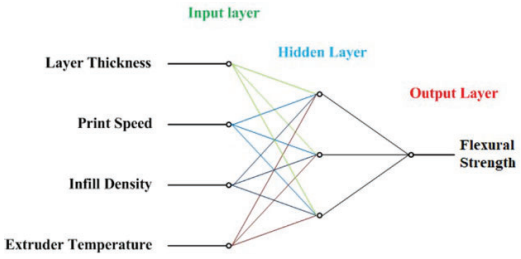

Fig. 6: ANN Architecture

The weights and biases discovered between the input and hidden layers are summarized in Table 4.. The biases and weights between hidden layer are $(BIAS)_w$ = -0.11812, X_w = -0.27521, Y_w = -1.0514, Z_w = -0.43481. Furthermore, R-sq has a value of 0.99.

Table 4. Weights for the input and hidden layers

	A_k	B_k	C_k	D_k	$(BIAS)_k$
X	-14.5503	15.192	5.5153	17.6814	-1.0468
Y	11.0571	18.3239	-9.9293	-14.3456	-6.154
Z	-2.6404	-9.6411	15.4334	-34.2633	5.9193
k varies from X to Z					

5.4 Mathematical Expression for ANN

The weights generated using the approach described by Shrivastava et al.[21] have been examined in order to create the mathematical model[22]. With the formulae 2 and weights collected from the input and hidden layers, we can calculate the intermediate variable 'm.' Additionally, the first hidden layer's value of neurons was computed by applying the formulae 3. The equation 4 is used to determine the intermediate variable (n) that exists in between hidden and output layers.

$$m_X = A_X \times A + B_X \times B + C_X \times C + D_X \times D + BIAS_X$$
$$m_Y = A_Y \times A + B_Y \times B + C_Y \times C + D_Y \times D + BIAS_Y$$
$$m_Z = A_Z \times A + B_Z \times B + C_Z \times C + D_Z \times D + BIAS_Z \quad (2)$$

$$X = \frac{2}{[1+\exp(-2\times m_X)}-1$$

$$Y = \frac{2}{[1+\exp(-2\times m_Y)}-1$$

$$Z = \frac{2}{[1+\exp(-2\times m_Z)}-1 \quad (3)$$

$$n_W = X_W \times X + Y_W \times Y + Z_W \times Z + BIAS_W \quad (4)$$

$$W = \frac{2}{[1+\exp(-2\times n_w)}-1 \quad (5)$$

As can be seen in equation 5, the mathematical model has been created by applying the expressions from equation 4.

5. Results and Discussion

It's possible to forecast flexural strength values using Equation 5. Flexural strength is shown in Table 5 as predicted and experimental results. Equation 6 has been used to calculate the percentage deviation[23].

$$Percent\ deviation = \frac{Experimental\ value - Predicted\ Value}{Experimental\ Value}\ X\ 100 \quad (6)$$

Figure 7 shows how values derived from experiments differ from those based on predictions. The percentage variation is determined and shown in Table 5. The average percentage deviation for the ANN model is found to be 4.06 percent, which means the percentage deviation seems to be much lower for this model. It also appears that as the ANN model has a better R-sq value as compared to the regression model, hence, by altering the input parameters, the ANN model can predict changes in flexural strength quite accurately.

Table 5. ANN Predicted values and percentage deviation

S. No.	A	B	C	D	Experimental values	Predicted values	% Deviation
1	0.20	50	70	190	14.632	14.362	1.88
2	0.20	100	80	200	11.836	11.836	0.00
3	0.20	150	90	210	15.146	15.146	0.00
4	0.20	200	100	220	16.113	15.503	3.75
5	0.25	50	80	210	15.962	15.915	0.29
6	0.25	100	70	220	14.978	15.503	3.14
7	0.25	150	100	190	3.193	3.889	21.81
8	0.25	200	90	200	1.729	2.078	15.65
9	0.30	50	90	220	17.051	16.474	3.45
10	0.30	100	100	210	12.187	12.187	0.00
11	0.30	150	70	200	6.006	6.031	0.41
12	0.30	200	80	190	2.988	2.732	11.47
13	0.35	50	100	200	14.039	14.362	2.26
14	0.35	100	90	190	2.754	2.732	0.75
Average percentage deviation						4.06 %	

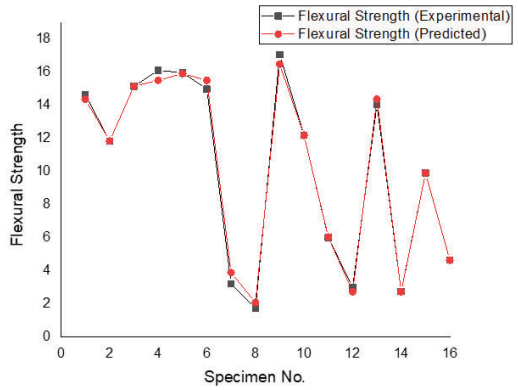

Fig. 7: Experimental versus Predicted values for ANN Model

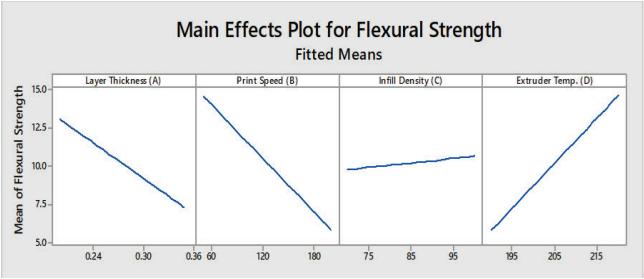

Fig. 8: Main Effect plot for Flexural Strength

In order to estimate the flexural strength value for any given combination of factors, we created a mathematical model based on regression analysis. The main effect plot[24] has been created (Fig. 8) for flexural strength in order to better comprehend the impact of several parameters on the final result, namely the flexural strength. Increasing layer thickness and print speed both decrease flexural strength while increasing infill density and extruder temperature increase it.

When printing a part, the thickness of a layer directly affects the number of layers needed and amount of time required for printing. Costs of production therefore fall as the thickness of the layer grows. A greater extrusion pressure is required to form a thin layer in order to enhance the bonding between layers, thus increasing the flexural strength. As long as the thickness of each layer is kept at a minimum, the quantity of layers will grow along with the ductility, leading to an increase in flexural strength. As printing speed increases, there is less time for solidification, and the adhesion between successive layers degrades, leading to a decrease in flexural strength.

Additionally, as the specimen mass grows with greater infill density leads to greater flexural strength. Increasing the temperature of the extruder provides optimal filament melting, resulting in smoother flow and enhanced adhesive qualities. hence increasing the tensile strength. Taguchi study revealed that the highest value of flexural strength may be achieved at infill density of 100 % , speed of print at 50 mm/sec, extruder temperature of 220 ^{0}C and layer thickness of 0.2 mm. To verify this, a sample has been printed for the aforementioned parametric values, and the flexural strength is the highest at 19,386 kg/mm^2.

6. Conclusions

The goal of the current research is to discover the input parameter values that provide the highest flexural strength for PLA samples printed on FDM-based printer. The samples are made with the L16 orthogonal design in mind. The regression and ANN models are further developed using the flexural strength measured values. The following are the study's major conclusions:

1. The regression analysis indicates that among the studied input parameters, extruder temperature, speed of print and layer thickness are critical variables which influence the flexural strength.
2. The regression's R-square value is 86.08 % while that of ANN is 99% with average percentage deviation under 5 percent, indicating that ANN model can be used to predict the values of flexural strength for any given set of input variables efficiently.
3. Taguchi studies indicates that the maximum flexural strength may be attained at an extruder temperature of 220 degrees Celsius, a layer thickness of 0.2 millimetres, a 100 percent infill density, and a print speed of 50 millimetres per second.
4. ANN model has confirmed that the acquired value of flexural strength is the highest among the parameters determined from Taguchi analysis, as evidenced by the validation result.

Nomenclature

PLA	Poly Lactic Acid
FDM	Fused Deposition Modelling
FFF	Fused Filament Fabrication
ANN	Artificial Neural Network

References

1) S. Scott Crump, "APPARATUS AND METHOD FOR CREATING THREE-DIMENSIONAL OBJECTS," 1992. doi:10.2116/bunsekikagaku.28.3_195.
2) S.K. Dhinesh, S. Arun Prakash, K.L. Senthil Kumar, and A. Megalingam, "Study on flexural and tensile behavior of pla, abs and pla-abs materials," *Mater. Today Proc*., 45 (xxxx) 1175–1180 (2021). doi:10.1016/j.matpr.2020.03.546.
3) S. Singh, G. Singh, C. Prakash, S. Ramakrishna, L. Lamberti, and C.I. Pruncu, "3D printed biodegradable composites: an insight into mechanical properties of pla/chitosan scaffold," *Polym. Test*., 89 (2020). doi:10.1016/j.polymertesting.2020.106722.
4) M.D. Zandi, R. Jerez-Mesa, J. Lluma-Fuentes, J.J. Roa, and J.A. Travieso-Rodriguez, "Experimental analysis of manufacturing parameters' effect on the flexural properties of wood-pla composite parts built through fff," *Int. J. Adv. Manuf. Technol*., 106 (9–10) 3985–3998 (2020). doi:10.1007/s00170-019-04907-4.
5) M. Günaya, "Modeling of tensile and bending strength for pla parts produced by fdm," *Int. J. 3D Print. Technol. Digit. Ind*., 3 (3) 204–211 (2019).
6) J.C. Camargo, Á.R. Machado, E.C. Almeida, and E.F.M.S. Silva, "Mechanical properties of pla-graphene filament for fdm 3d printing," *Int. J. Adv. Manuf. Technol*., 103 (5–8) 2423–2443 (2019). doi:10.1007/s00170-019-03532-5.
7) S.R. Rajpurohit, and H.K. Dave, "Flexural strength of fused filament fabricated (fff) pla parts on an open-source 3d printer," *Adv. Manuf*., 6 (4) 430–441 (2018). doi:10.1007/s40436-018-0237-6.
8) A.W. Gebisa, and H.G. Lemu, "Investigating effects of fused-deposition modeling (fdm) processing parameters on flexural properties of ultem 9085 using designed experiment," *Materials (Basel).,* 11 (4) 1–23 (2018). doi:10.3390/ma11040500.
9) J.M. Chacón, M.A. Caminero, E. García-Plaza, and P.J. Núñez, "Additive manufacturing of pla structures using fused deposition modelling: effect of process parameters on mechanical properties and their optimal selection," *Mater. Des*., 124 143–157 (2017). doi:10.1016/j.matdes.2017.03.065.
10) R. Hernandez, D. Slaughter, D. Whaley, J. Tate, and B. Asiabanpour, "Analyzing the tensile, compressive, and flexural properties of 3d printed abs p430 plastic based on printing orientation using fused deposition modeling," *Solid Free. Fabr. 2016 Proc. 27th Annu. Int. Solid Free. Fabr. Symp.* - An Addit. Manuf. Conf. SFF 2016, 939–950 (2016).
11) A.K. Sood, R.K. Ohdar, and S.S. Mahapatra, "Parametric appraisal of mechanical property of fused deposition modelling processed parts," *Mater. Des*., 31 (1) 287–295 (2010). doi:10.1016/j.matdes.2009.06.016.
12) M. Singh, and P.S. Bharti, "Parametric influence of process parameters on the wear rate of 3d printed polylactic acid specimens," *Indian J. Pure Appl. Phys*., 59 (03) 244–251 (2021).
13) A.K. Srivastava, M. Maurya, A. Saxena, N.K. Maurya, and S.P. Dwivedi, "Statistical optimization by response surface methodology of process parameters during the cnc turning operation of hybrid metal matrix composite," *Evergreen*, 8 (1) 51–62 (2021). doi:10.5109/4372260.
14) S.P. Dwivedi, N.K. Maurya, and M. Maurya, "Assessment of hardness on aa2014/eggshell composite produced via electromagnetic stir casting method," *Evergreen*, 6 (*4*) 285–294 (2019). doi:10.5109/2547354.
15) S.K. Deb, N. Deb, and S. Roy, "Investigation of factors influencing the choice of smartphone banking in bangladesh," *Evergreen*, 6 (*3*) 230–239 (2019). doi:10.5109/2349299.
16) A. Kumar, A.K. Chanda, and S. Angra, "Optimization of stiffness properties of composite sandwich using hybrid taguchi-gra-pca," *Evergreen*, 8 (2) 310–317 (2021). doi:10.5109/4480708.
17) P.K. Shrivastava, and A.K. Pandey, "Geometrical quality evaluation in laser cutting of inconel-718 sheet by using taguchi based regression analysis and particle swarm optimization," *Infrared Phys. Technol.,* 89 369–380 (2018). doi:10.1016/j.infrared.2018.01.028.
18) M.I. Alhamid, N. Nasruddin, Budihardjo, E. Susanto, T.F. Vickary, and M. Arif Budiyanto, "Refrigeration cycle exergy-based analysis of hydrocarbon (r600a) refrigerant for optimization of household refrigerator," *Evergreen*, 6 (*1*) 71–77 (2019). doi:10.5109/2321015.
19) N. Weake, M. Pant, A. Sheroan, A. Haleem, and H. Kumar, "Optimising process parameters of fused filament fabrication to achieve optimum tensile strength," *Procedia Manuf*., 51 (3) 704–709 (2020). doi:10.1016/j.promfg.2020.10.099.
20) Y. Shrivastava, and B. Singh, "Stable cutting zone prediction in computer numerical control turning based on empirical mode decomposition and artificial neural network approach," *Trans. Inst. Meas. Control*, 41 (*1*) 193–209 (2019). doi:10.1177/0142331218757285.
21) Y. Shrivastava, and B. Singh, "Stable cutting zone prediction in cnc turning using adaptive signal

processing technique merged with artificial neural network and multi-objective genetic algorithm," *Eur. J. Mech. A/Solids*, 70 238–248 (2018). doi:10.1016/j.euromechsol.2018.03.009.

22) T.N. Dief, and S. Yoshida, "System identification for quad-rotor parameters using neural network," *Evergreen*, 3 (*1*) 6–11 (2016). doi:10.5109/1657380.
23) M. Sultan, I.I. El-Sharkawl, T. Miyazaki, B.B. Saha, and S. Koyama, "Experimental study on carbon based adsorbents for greenhouse dehumidification," *Evergreen*, 1 (*2*) 5–11 (2014). doi:10.5109/1495157.
24) S. Choudhary, A. Sharma, S. Gupta, H. Purohit, and S. Sachan, "Use of rsm technology for the optimization of received signal strength for lte signals under the influence of varying atmospheric conditions," *Evergreen*, 7 (*4*) 500–509 (2020). doi:10.5109/4150469.
25) S.K. Deb, N. Deb, and S. Roy, "Investigation of factors influencing the choice of smartphone banking in bangladesh," *Evergreen*, 6 (*3*) 230–239 (2019). doi:10.5109/2349299.